This paper was published as : C.F. Reinhart, M. Andersen, Development and validation of a Radiance model for a translucent panel, Energy and Buildings, vol. 38 (7), pp. 890-904, 2006.

Development and validation of a Radiance model for a translucent panel

Christoph F. Reinhart [a *], Marilyne Andersen [b#]
[a] Institute for Research in Construction
National Research Council Canada, Ottawa, Ont., K1A 0R6, Canada
[b] Solar Energy and Building Physics Laboratory (LESO-PB)
Swiss Federal Institute of Technology (EPFL), Switzerland

Abstract

This study describes the development and validation of a Radiance model for a translucent panel. Using goniophotometer data combined with integrating sphere measurements, optical properties of the panel were derived and converted into a Radiance model using the *trans* and *transdata* material types. The Radiance model was validated in a full scale test room with a facade featuring the translucent panel material. Over 120,000 desktop and ceiling illuminances under 24,000 sky conditions were measured and compared to simulation results using the Perez sky model and a Radiance-based daylight coefficient approach. Overall mean bias errors (MBE) below 9% and root mean square errors (RMSE) below 19% demonstrate that translucent materials can be modeled in Radiance with an even higher accuracy than was demonstrated in earlier validation studies for the *plastic*, *metal*, and *glass* material types. Further analysis of results suggests that the accuracy of around ±20% currently reached by dynamic Radiance/Perez/daylight coefficient calculations for many material types is sufficient for practical design considerations. A procedure is described showing how goniophotometer

* Corresponding author: email: christoph.reinhart@nrc.ca; Tel. +1(613)993-9703
# Current address: Building Technology Program, Department of Architecture, Massachusetts Institute of Technology (MIT), USA

and integrating sphere measurements can be used to accurately model arbitrary translucent materials in Radiance using *transdata* function files.

keywords: Radiance/Daysim validation, translucent glazings, complex fenestration systems, goniophotometer, BTDF, BRDF, integrating sphere

1 Introduction

Daylight simulations are computer-based calculations of interior lighting conditions due to daylight. Such calculations can be used during building design to quantitatively compare different design options. A recent online survey of 185 designers, engineers and researchers from 27 countries on the ”use of daylight simulation during building design” established that (a) a growing number of design practitioners nowadays routinely uses daylight simulations to predict daylight factor and interior illuminance distributions and (b) that trust in the reliability of daylighting tools has risen compared to earlier surveys[1]. While survey participants named over forty different daylight simulation programs that they routinely used, over 50% of all program selections were for tools that use the Radiance simulation engine[2]. Radiance is a backward raytracer that was originally developed by Ward at Lawrence Berkeley National Laboratories. Ongoing developments involve a network of individuals and institutions worldwide (http://www.radiance-online.org/).

What is the attraction of Radiance over competing daylight simulation engines? One often cited quality of Radiance is that it is *physically based* and capable of simulating complex geometries with flexible reflection and transmittance material properties using a mixed stochastic, deterministic backward raytracing algorithm[3]. The ability to model specular components constitutes an advantage over radiosity based simulation

approaches which treat all surfaces as Lambertian diffusers. Radiance's scientific reputation is further founded on a series of independent validation studies.

A rigorous validation study of a simulation algorithm should quantify how closely simulation predictions resemble physical measurements. Accordingly, a number of previous Radiance validation studies compared measurements of interior daylight illuminances under multiple sky conditions to illuminances simulated with Radiance. The results of these studies largely depended on whether exterior sky conditions were *measured* using a sky scanner or *modeled* based on a sky model.

Between 1995 and 2000 Mardaljevic published a series of three papers[4-6] that used measurements of interior illuminances and compared them with Radiance simulations based on sky scanner data that had been collected synchronously. The data set, collected by Aizlewood[7] at the Building Research Establishment (BRE), was chosen so that "simulation errors that are solely caused by the Radiance lighting algorithm without being further compromised by errors in the representation of the sky"[4] could be determined.

In his first study, Mardaljevic[4] considered a facade with a clear single pane glazing with and without an internal lightshelf. The window pane was modeled as a Radiance *glass* material. Diffuse and specular lightshelves were modeled as *plastic* and *mirror* materials, respectively. Mardaljevic found that Radiance was capable of reliably modeling interior illuminances for clear and overcast sky conditions.

In 1997, Mardaljevic[5] presented further validation data from the BRE data set for the facade with a clear glazing under over 700 sky conditions. Again, he found "that Radiance could predict internal illuminances to a high degree of accuracy for a wide range of actual sky conditions" based on sky scanner data.

In 2000, Mardaljevic[6] presented a third Radiance validation study using the same data as in 1997 but combining Radiance with a daylight coefficient[8] approach to simulate indoor illuminance more effectively. He found that daylight coefficient based Radiance simulations "should be considered almost equivalent in accuracy to the standard [time-step by time-step] calculation"[6].

Sky scanner data are rare and generally not publicly available. This scarcity of sky scanner data forces most daylight simulators to use a sky model as a starting point for their simulations. Frequent choices for a sky model are the "old" CIE overcast and clear skies[9]. The CIE overcast sky is particularly popular as it serves as the reference sky for daylight factor calculations. A limitation of CIE overcast is that its input is limited to a single scaling factor on a fixed distribution. This limitation is the reason why in a study conducted in 2000, that compared different dynamic Radiance-based daylight simulation methods, the ones based on the CIE sky model performed consistently worse than methods based on the all weather Perez sky model[10].

In 2001, Ng[11] used the CIE overcast sky for a Radiance and Lightscape validation study of outside facade illuminances in a dense urban setting in Hong Kong. The study's underlying assumption was that "the relative error between a cloudy sky in Hong Kong and the CIE overcast sky is small"[11]. Ng found that both investigated simulation programs overestimated the daylit illuminance on a highly obstructed facade by over 50% – a modest result given the performance attested to Radiance in earlier validation studies.

As a follow up to Ng's work, Mardaljevic[12] wrote a discussion on "assumptions commonly made in validation studies for lighting simulation programs". The paper revealed substantial discrepancies between the luminous distribution of most measured, seemingly overcast sky conditions in the BRE-IDMP data set and the CIE overcast sky.

When reproducing the filtering criteria used by Ng to decide whether a sky condition was cloudy, stable, and sufficiently bright, most remaining BRE-IDMP overcast skies were still not closely matching the CIE overcast sky. Much more stringent filtering criteria were required to ensure similarity between measured skies and CIE overcast. The second part of the paper explored simulation errors arising from choosing incorrect reflectance values for obstructing facades. The paper concluded with a compelling argument, that the poor performance of Radiance in the Hong Kong study probably resulted from errors in the simulation model (CIE overcast sky condition and uncertainty in the effective reflectivity of textured building surfaces) rather than the intrinsic accuracy of Radiance[12]. The study concluded that one has to carefully watch external overcast sky conditions during measurements when using the CIE overcast sky for program validation.

What about dynamic sky models –such as Perez[13]– that require direct and diffuse irradiances as input? The “charm” of the Perez model from the practitioner’s point of view is that all inputs including hourly time series of direct and diffuse irradiances are available free-of-charge for multiple sites on earth as they form part of standard climate files[14]. This makes it tempting to use Perez combined with Radiance both in design practice as well as for validation studies. Given the unsatisfactory experiences that have been made with the CIE/Radiance combination, the question is whether Perez/Radiance can deliver better results.

Reinhart and Walkenhorst[15] measured internal illuminances and external direct and diffuse irradiances under over 10,000 sky conditions measured in 30 second intervals to validate a Radiance-based daylight coefficient approach combined with the Perez model. Internal illuminances were collected in a full scale test room with a SSW facing facade. The facade was fully glazed above the balustrade and featured an

external, partly specular venetian blind system. Three blind settings were considered. The researchers found that daylight autonomies for the investigated sky conditions could be predicted with a relative error below two percentage points and that simulation errors could be attributed to about equal parts to the Radiance algorithm and the Perez sky model. Mean bias errors were less than 6% for work plane sensors compared to 20% for ceiling sensors. The reason for this discrepancy between upward facing desktop sensors and downward facing ceiling sensors was that the latter are strongly influenced by the building's surroundings landscape and neighboring buildings. This finding went hand in hand with Mardaljevic's observation[12], that the ability to correctly model external ground and obstruction reflectances has a strong impact on the resulting simulation accuracy.

Which type of Radiance validation is more relevant: Radiance by itself or in combination with a reliable sky model such as Perez? The obvious fundamental limitation of the latter is that differences between measured and simulated interior illuminances stem from the *compound error* of the sky model and the lighting simulation algorithm. Therefore, one could rightfully argue, that a validation study starting with a sky model cannot quantify the *intrinsic* accuracy of the lighting simulation algorithm, as simulation results are partly corrupted by sky model errors, the size of which varies for different sky conditions. A contra-argument is that the compound error is ultimately what is of interest to a design practitioner, who wants to carry out an annual daylight simulation but who does not have sky scanner data to work with. Both positions are valid and have been presented here to sensitize the reader to the particular attention required to how the sky was modeled in any given daylight simulation study (research or design practice).

Summing up, the above described research makes a compelling case, that Radiance is capable of modeling interior illuminances due to daylight for a wide range of sky conditions and complex facade geometries (including venetian blinds). Radiance is further able to model a range of diffuse and specular reflecting real world materials and standard glazings. The Perez/Radiance combination leads to satisfying results in the absence of sky scanner data for a particular building site. If multiple sky conditions are to be considered, Radiance can be combined with a daylight coefficient approach to speed up the calculation without any significant penalty in the accuracy of the simulation.

This paper adds to the above described suite of Radiance validation studies by exploring the Radiance material types *trans* and *transdata*. All above described studies relied exclusively on the *plastic*, *metal*, and *glass* material types to model all surfaces in the investigated scenes. *Plastic* and *metal* model ideal Lambertian reflectors with a fixed specular component. *Glass* describes a thin glass surface and can be used to model standard single and double glazings. For materials that do not fall in any of these categories, Radiance offers a suite of further material types that characterize reflectance and transmittance properties with various degrees of detail. E.g. the *trans* model has been used in the past to approximate the optical properties of materials such as translucent panels[*] or thermotropic glazings[16]. The *trans* model treats a material as an ideally diffusing light transmitter with a fixed specular component. The light flux passing through a *trans* material as a function of incident angle is constant. Since the transmitted light flux of some real world materials decreases for rising incident angles, Radiance offers two more advanced material types, *transdata* or *transfunc,* which allow one to adjust the transmittance properties of the material according to measured data. To date,

[*] for example see: http://www.advancedglazings.com/expSolera/radiance.php

no rigorous validation study has been carried out for either of the three translucent Radiance material types, *trans*, *transfunc*, or *transdata*. To close this gap the objectives of this study are:

(a) to increase the number of validated Radiance material types,

(b) present a methodology of how to derive a Radiance material model of a translucent panel based on goniophotometer and integrating sphere measurements,

(c) to validate the resulting Radiance model in a full scale test room, and

(d) to explore how significant remaining simulation errors are for practical design considerations

2 Methodology

To address the study's objectives, the following four steps were carried out:

- Optical measurements: A series of goniophotometer and integrating sphere measurements were performed to fully characterize the optical properties of a commercially available translucent sandwiched panel, illustrated in Figure 1. The translucent panel system consisted of two 300 mm x 300 mm UV-stabilized Fiberglass reinforced Polyester facesheets and was filled with a 78 mm thick white glass wool type of insulation[17].
- Development of a Radiance model: The resulting bidirectional reflection and transmission distribution functions (BRDF and BTDF i.e. ratio of the luminance emerging from the sample after either reflection or transmission and incident illuminance on the sample plane) were used together with angle-dependent direct hemispherical transmittances to deduce two basic *trans* models and a more advanced *transdata* Radiance model of the translucent panel.

- Test-room measurements: In parallel, measurements of internal illuminances in a full scale test room equipped with the same type of translucent panel were collected together with external direct and diffuse irradiances.
- Radiance/Perez validation: Daylight simulations using the formerly developed Radiance material models combined with the Perez sky model were compared to the test room measurements.

The rest of this section describes these individual steps in detail.

2.1 Optical measurements

2.1.1 Goniophotometer Measurements

To develop a Radiance material that reproduces the optical properties of the selected translucent sample faithfully, its bidirectional light distribution function must first be determined in transmission (BTDF) and reflection (BRDF), so that the spatial distribution of emerging light can be identified for varying incident directions. Goniophotometer measurements were carried out for this purpose at the Solar Energy and Building Physics Laboratory (LESO-PB) of the Swiss Federal Institute of Technology in Lausanne (EPFL) with an instrument based on digital imaging techniques, comprising a rotating diffusing screen on which the emerging light flux is collected and reflected towards a digital video-camera (CCD), used as a multiple-points luminance-meter[18].

The objectives of these measurements were two-fold. On one hand, they aimed at defining the overall light transmission distribution for different incident directions. More specifically, the goal was to either verify that light transmission was sufficiently diffuse so that variations in transmitted luminance could not be easily detected by the human eye or, if this proved not to be the case, to find what transmission function would be able to

simulate the measured behavior in Radiance. The second objective was to determine the directional-hemispherical transmittance and reflectance for different incident angles, based on an integration of BTDFs and BRDFs over the full collection hemisphere, and adjust the corresponding Radiance material description accordingly.

Bidirectional measurements were taken in both transmission (BTDF) and reflection (BRDF) modes. Preliminary BTDF and BRDF measurements were conducted with an illuminated area of diameter 150 mm on the exterior side of the system and a second diaphragm of diameter 280 mm on the interior side to minimize the corners' effect. They revealed a rotationally invariant transmission pattern but also a low directional-hemispherical transmittance (around 20%) and hence extremely low BTDF values even at normal incidence (< 0.09 cd m^{-2} lux^{-1}). It was therefore decided to use a larger illuminated area of diameter 280 mm for transmission measurements to keep a reasonable signal to noise ratio despite the fact that stronger edge effects would be likely to occur, the material sample being only slightly larger (300 mm by 300 mm) than this area. However, as the sample is highly volume-scattering due to the 'angel-hair' filling within the two fiberglass layers and mounted in a brushed metal (reflective) enclosure, these effects were expected to be at least partially compensated and light loss reduced.

For reflection measurements, the smaller sample area, preferable for directional accuracy reasons as explained below, could be kept because detected luminance values were much higher (> 2 cd m^{-2} lux^{-1}). Reflection measurements were used to (a) estimate the direct-hemispherical reflectance of the material, required for a complete description of the material for the Radiance model, and (b) to detect any irregular reflectance features.

From the BTDF or BRDF values determined for each pixel on the calibrated screen images, a finite bidirectional dataset was generated according to an averaging grid[19] presenting given angular intervals in altitude and azimuth. These intervals had to be

chosen consistently with the illuminated sample area: as light rays emerging from the sample and reaching a given pixel could potentially come from anywhere within the sample emitting area, there is a range of emerging directions associated with a pixel. To account for this, the averaging sectors had to be chosen so that they cover angular intervals of extent comparable to this range[21], which makes directional accuracy inversely proportional to sample size.

Although a larger sample area was necessary for transmission measurements because of the low luminance levels (280 mm, which led to angular intervals of 15° in altitude and 20° in azimuth), a finer angular resolution was preferred for the BRDF data (every 5° in altitude and 15° in azimuth) and hence a smaller sample area (150 mm in diameter) was chosen for these measurments. The results' reliability could be maintained thanks to larger luminance values in reflection. The incident directions set for BTDF measurements consisted of altitude angles 0° (normal incidence), 15°, 20°, 30°, 40°, 45°, 60° and 75° along azimuth planes C0 and C90 (15 incident directions in total); for BRDF measurements, only altitudes every 20° were considered (0°, 20°, 40°, 60°) for these two azimuth planes (C0 and C90), leading to 7 directions in reflection mode.

Figure 2 displays the resulting BTDF and BRDF data as photometric solids and section views[20], plotted in spherical coordinates for some of the investigated incident directions. Measurement errors are estimated to be of about 10% to 15%, based on an extensive validation study conducted for that particular goniophotometer[21].

As can be observed on Figures 2(a) to 2(e), light is transmitted in a diffuse way independently of the incident angle: BTDFs exhibit a rotational symmetry for normal incidence that is maintained along the normal emerging direction even for growing incident altitudes, with relative fluctuations of $\pm$15%; furthermore, there is no difference

between BTDF values obtained along the C0 and C90 planes. Due to the particularly low BTDF values (ranging between 0.08 cd m^{-2} lux^{-1} for normal incidence down to 0.01 cd m^{-2} lux^{-1} for grazing incidence (75° from normal), it was expected that experimental errors would be larger than the 10% predicted by the validation study, and the observed 15% error was still considered satisfactory given that slight manufacturing imperfections or mechanical adjustments also strongly influence the results.

BRDF results (Fig. 2(f)) initially seemed to suggest that light is reflected mainly along the specular direction, with a small diffuse component around it due to the bulk scattering taking place within the central layer of the panel. A more careful analysis of the BRDF functions yielded a mean specular reflectance of about 8% (assuming a cone centered around the specular peak with an opening half-angle of 15°) and a mean diffuse reflectance of 21% (the measured direct-hemispherical reflectances ranged from 27% to 31% for the different incident directions). This result was surprising to the authors given the visual impression one gets from Figure 2(f). The reason for this seeming discrepancy was that even very small reflectances along many directions can make up a significant sum.

As far as the direct-hemispherical transmission is concerned, it was found to decrease consistently when the incident altitude increased, according to the curve shown in Figure 3. As a matter of fact, a hexagonal symmetry could be discerned when BTDF values start being lower than 0.04 cd m^{-2} lux^{-1}, as in Figures 2(b), 2(d) and 2(e). This is a sign that detected light levels become close to the limit (minimal) luminances still accurately captured by the CCD camera (estimated at 0.015 cd m^{-2} emitted from the screen[21]): indeed, the assessment method itself, based on a combination of 6 adjacent projection screen positions[18], then becomes faintly apparent, which means that the

correction and calibration factors applied to the detected screen luminances are not able to compensate fully for the device's particular geometry anymore. This would have been exacerbated with the smaller (150 mm diameter) sample area, which, again, confirms the necessity for the chosen, larger illuminated area and therefore coarser measurement set.

As direct-hemispherical transmittance values are critical in defining the corresponding material model in Radiance (section 2.2), and as the above described analysis of the transmission figures suggested that the experimental conditions were reaching the limits of the instrument's measurement capabilities, a complimentary set of measurements was carried out with an integrating sphere, so that the transmittance data could be verified and accuracy could be ensured.

2.1.2 Integrating Sphere Measurements

Angle-dependent direct hemispherical light transmittances of the same sample were determined using an integrating sphere at the Fraunhofer Institute for Solar Energy Systems (ISE), Germany. The integrating sphere, of diameter 0.65 m, was coated with a 10 mm thick, highly diffuse custom-made PTFE-layer (volume scattering). The light source was a 2.5 kW HMI lamp, whose beam was first collected by a CPC (Compound Parabolic Collector), the outlet of which was covered with a diffusing low-iron glass pane (sand-blasted). A series of diaphragms was then used to restrict the irradiated surface of the sample to about 500 mm in diameter. Light emerging on the other side of the sample was restricted to 100 mm, which corresponded to the diameter of the entrance port of the Ulbricht sphere. The photodetector consisted of a pyroelectric (pin-diode) radiometer and a diode-array spectrometer equipped with a V(λ)-correction filter. Based on previous

measurements conducted with scattering samples, an experimental error of 5% was reported by the Fraunhofer ISE for the integrating sphere data.

The angle of incidence was varied from 0° to 75° in steps of 5°. The hemispherical reflectance of the back of the sample for incident diffuse radiation (originating from the integrating sphere) was determined for the sample with the Diffuse Radiation Source (DRS) using a sample port aperture of 10cm diameter. This value was needed for the second order correction stemming from the change of sphere throughput due to the sample at the measurement port.

The results from the integrating sphere measurements are shown in Figure 3 (solid line). As can be observed on this graph, goniophotometer-based direct-hemispherical transmittances were consistently lower than integrating sphere results, but error bars generally overlapped each other except for incident angles of 60° and higher. Based on the lower error estimate for integrating sphere values and on the previously observed fact that the goniophotometer was likely reaching its limits in terms of accuracy, it was decided to use the sphere's direct-hemispherical transmittance data for the Radiance model of this translucent panel. However, given the satisfactory agreement between both datasets, the conclusions drawn from the goniophotometer dataset describing the general behavior in transmission and reflection of this material were still considered valid, and were used in defining its simulated optical properties.

Summing up, the main conclusions that were drawn from the goniophotometer and integrating sphere measurements of the translucent sandwich system were:

(a) The system is rotationally invariant (no variation with either the incident or the emerging azimuth angles).

(b) Given that the BTDF data exhibits no correlation with the incident direction and that its photometric solid approaches the shape of a hemisphere within an error margin of ±15% (Figures 2(a) to 2(e)), the investigated system can be treated for simulation purposes as an ideal diffuser.

(c) The directional-hemispherical transmittance of the system decreases according to the solid line in Figure 3 when incidence moves closer to grazing angles, with a maximal transmittance at normal incidence equal to 0.24.

(d) The panel has diffusing and specular reflectances of 0.21 and 0.08, respectively.

2.2 Development of a Radiance model

Based on the analysis of the previous section, three Radiance materials of varying complexity were developed for the translucent panel using the *trans* and *transdata* material models:

trans$_{24\%}$ model: According to page 325 of the *Rendering with Radiance*[2] book the *trans* material is "...one of the most confusing material entities in the Radiance repertoire. However, it is the simplest material that will trace direct source rays through a semispecular surface in order to determine diffuse and specular transmitted components...". Using *trans,* Radiance treats the translucent panel as a perfect Lambertian diffuser with diffusing and specular reflectances of 0.21 and 0.08, respectively. The *trans* model further assumes that the directional hemispherical transmittance is constant for different incidence angles, i.e. it approximates the solid line in Figure 3 with a constant. Which constant a simulationist chooses obviously depends on his or her knowledge of the curve in Figure 3. In the case that only direct normal hemispherical transmittance measurements were carried out, the curve in Figure 3 would

be approximated with a constant value of 0.24. This would result in the following material model:

```
# RADIANCE "trans" model of a translucent panel assuming
# only direct normal hemispherical transmittance is available
# Rd = Cr = Cg = Cb = 0.21 = diffuse reflectance
# Rs = A4 =0.08 = specular reflectance
# Sr = 0.0 = surface roughness
# Td = 0.24 = direct normal diffuse hemispherical transmittance
# Ts = 0 = transmitted specularity (ideal diffuser)
# A7 = Ts/(Td+Ts) = 0
# A6 = (Td+Ts)/(Rd+Td+Ts) = 0.5333
# A5 = Sr = 0
# A1 = A2 =A3 = Rd/((1-Rs)*(1-A6)) = 0.48913
# St = A6*A7*(1-A1)*A4 = 0
# resulting Radiance material:
void trans PANEL
0
0
7 0.48913 0.48913 0.48913 0.08 0  0.5333 0
# A1      A2      A3      A4   A5 A6     A7
```

trans$_{16\%}$ model: A look at Figure 3 shows that approximating the solid line with a constant of 0.24 will lead to an overestimation of indoor illuminances. Given that diffuse daylight is usually incident onto a panel under all possible incident directions, it seems advisable to replace the 0.24 direct normal hemispherical transmittance with the diffuse-diffuse transmittance, $T_{diffuse\text{-}diffuse}$, of the sample which is defined as[22]:

$$T_{diffuse\text{-}diffuse} = \int_{\theta=0}^{\frac{\pi}{2}} T(\theta)\sin(2\theta)d\theta$$

where θ is the incident angle. For the sample, the diffuse-diffuse transmittance corresponds to 0.1621. Following the same calculations as above but using 0.1621 instead of the 0.24 for the total transmittance leads to the following Radiance model:

```
# RADIANCE "trans" model of a translucent panel based on a
# diffuse-diffuse transmittance of 0.1621.
void trans PANEL
0
0
7 0.40446 0.40446 0.40446 0.08 0  0.435635 0
```

```
# A1        A2        A3        A4    A5  A6        A7
```

One should note that by using the diffuse-diffuse transmittance one is effectively weighing incident rays from all directions equally which is strictly speaking only valid for a uniform diffuse sky.

transdata model: As discussed above, *trans* approximates the angle-dependant direct hemispherical transmittance with a constant. To overcome this limitation, the *transdata* model allows one to specify a custom tailored angular dependency for transmitted light. Unfortunately, this corrective function is only applied to direct ”light” sources, i.e. direct sunlight, whereas “glow” light sources –such as diffuse daylight– are still subject to a constant transmittance value. I.e. for diffuse daylight *transdata* and *trans* become identical. Using the solid curve from Figure 3 and a diffuse-diffuse transmittance of 0.1621 leads to the following *transdata* Radiance material[#]:

```
# RADIANCE “transdata” model of a translucent panel
void transdata PANEL
4 noop refl.dat rang.cal rang
0
6 0.40446 0.40446 0.40446 0.08 0.435635 1
```

The function file "rang.cal" calculates the angle “rang” between the direction of the incident light (dx,dy,dz) and the surface normal (Nx,Ny,Nz):

```
{ Compute incident angle in degrees (from either side) }
rang(dx,dy,dz) = 180/PI*Acos(abs(Nx*dx+Ny*dy+Nz*dz));
```

“rang” is the coordinate index for the data file "refl.dat" which contains corrective values for “rang” values between 0 and 90 degrees[%]:

[#] Thanks to Greg Ward for helping to put this function together.

[%] As explained in the Radiance help files, function files such as refl.dat and rang.cal should be copied into the

```
# integrating sphere measurements
##### HEADER #####
# one-dimensional data array
1
# irregularly spaced axis:
# two zeros – number of divisions – division values
0 0 17
0 5 10 15 20 25 30 35 40 45 50 55 60 65 70 75 90
##### Body #####
# Data values:
0.4713
0.4674
0.4615
0.4497
0.4359
0.4183
0.3986
0.3770
0.3534
0.3279
0.3024
0.2749
0.2494
0.2239
0.1983
0.1669
0
```

The data values in "refl.dat" were generated as the ratio of measured total transmittances. E.g. for 45^{o} the panel had a total transmittance of 0.167 (see Figure 3) resulting in a correction factor of:

$$\frac{\text{transmittance}_{\text{mea}}}{\text{transmittance}_{\text{constant}}} = \frac{\frac{0.167}{\pi}}{0.1621} = 0.3279$$

Radiance library directory. A description of Radiance data files can be found under http://radsite.lbl.gov/radiance/ Reference>> Documents >> File Formats (last accessed Feb 2006).

2.3 Test room measurements

For the validation part of this study, a facade featuring a large sample of the translucent panel investigated above was installed in one of the two identical test rooms of the NRC daylighting laboratory in Ottawa, Canada (45.32^{o}N, 75.67^{o}W) (Figure 4). The facade of the test rooms is facing SSE (25.2^{o} from due South). The two test rooms are both full scale (2.85m x 4,5m x 2.96m) and each is equipped with twelve Licor illuminance sensors that are mounted at identical positions in the rooms. The measurement error for the illuminance sensors was assumed to be 5%. For this study five of the illuminance sensors (two desktop and three ceiling) were considered (Figure 5). Outdoor direct and diffuse irradiances were synchronously collected every 30 seconds using a Yankee rotating shadowband radiometer.

Figure 4(a) shows an interior view of the investigated facade. A small tinted double-glazed window was placed in the center of the facade to act as a visual link to the outside for a series of research participants that spent several working days in the test rooms. The results of the human subject studies were not related to the work presented in this study and will be reported elsewhere. The involvement of human subjects further necessitated that the immediate exterior vicinity exterior of the NRC daylighting laboratory was visually separated from the building surroundings using a hedge (Figure 4(b)). This hedge was introduced to give test subjects an enhanced feeling of privacy when working in the test rooms. For the duration of the validation measurement, the hedge was covered with a black cloth to reduce errors in the Radiance scene such as inaccurate reflectances from the ground and surrounding objects.

Interior illuminances were continuously collected every 30 seconds over a period of nineteen days from May 4th 2004 until June 3rd 2004. During the nineteen days sky conditions ranged from overcast to partly cloudy and sunny. Measurements were only

considered for the validation study if the measured illuminance on the SSE facade of the test room was above 5000 lux. This selection criteria was used since the Perez sky model (or any other sky model) becomes extremely sensitive to measurement uncertainties of input direct irradiances just after sunrise or before sunset. This can translate into very large relative simulation errors at times which are not really significant for an annual daylight simulation since interior illuminances are only in the order of 50 to 100 lux. The 5000 lux filtering procedure resulted in a total of 24,252 valid sky conditions and over 120,000 measured interior illuminances.

2.4 Radiance/Perez validation

Daylight simulations were carried out using the Radiance-based daylighting analysis program Daysim. Daysim uses the Radiance algorithm combined with a validated daylight coefficient approach and the Perez sky model to simulate time series of indoor illuminances/luminances[15]. A detailed three dimensional AutoCAD model of the NRC daylighting laboratory and the surrounding hedge was made and converted into Radiance format. Based on simple measurements using a luminance meter, an illuminance meter, and a reference reflector, the approximate reflectances of walls, ceiling and floor were determined (Table 1). The visual transmittance of the tinted glazing was provided through integrating sphere measurements. The translucent material was modeled using either of the three models developed in section 2.2.

Table 2 presents a list of utilized Radiance simulation parameters. Only non default parameters are listed.

3 Results and Analysis

In this section the results of the model validation are presented and analyzed.

Cloudy Day

Figure 6 compares measurements and simulation results for a partly cloudy day for the desk sensor Desk1 located near the facade (*see* Figure 5). Since $trans_{16\%}$ and *transdata* yield identical results in the absence of direct sunlight, both simulation plots are shown as one. The figure shows that both Radiance models that assume a diffuse hemispherical transmittance of 0.1621 combined with the Perez sky model are capable of modeling the short time step development of indoor illuminances with a high degree of accuracy. In contrast, as one would expect, $trans_{24\%}$ predictions lie up to 40% above the measured values.

Sunny Day

Figure 7 shows the same results as Figure 6 on a sunny day for (a) the facade sensor and (b) desktop sensor Desk1. For the external sensor simulation results for $trans_{24\%}$, $trans_{16\%}$, and *transdata* are identical whereas they are markedly different for the desktop sensor. Figure 7(a) reveals that outside facade illuminances could be predicted with a high degree of accuracy throughout the day with some errors occurring at around at around 10.00 and 15.00. This suggests that the simulation errors introduced by the Perez sky model and surrounding landscape were small for the investigated day.

The results are markedly different for the desktop sensor (Figure 7(b)). At 10AM, $trans_{24\%}$ overestimated the desk illuminance by 44% while $trans_{16\%}$ and *transdata* both lie within a 5% error band with respect to the measured value. Why do the values for

trans$_{16\%}$ and *transdata* lie so close together for most of that sunny day? At 10AM the incident angle of the sun with respect to the translucent panel was around 55^{o}. According to Figure 3, the direct hemispherical transmittance at an incidence angle of 55% corresponds to 14% which is close but slightly under the diffuse-diffuse transmittance of 0.1621. Accordingly, t*rans*$_{16\%}$ and *transdata* lie close together at this time with the former being slightly larger than the latter. The same argument explains why the *trans*$_{24\%}$ value is around 1.5 (0.24/0.16) times larger than the measured value.

Comparing the measurements with *trans*$_{16\%}$ and *transdata* predictions, the values for the supposedly less detailed model (*trans*$_{16\%}$) lie slightly closer to the measurements than the more sophisticated model. The reason for this surprising finding might be coincidental: Given that at around 10AM the facade sensor simulation underestimated the measurement by 3%, suggests that errors related to the Perez sky model and surrounding landscape canceled themselves out with overpredictions caused by the *trans*$_{16\%}$ model.

MBE and RMSE

In order to provide a more rigorous analysis of the errors introduced by all three Radiance material models, the relative mean bias error (MBE) and the relative root mean square error (RMSE) with respect to the measurements were calculated for all three simulation sets. The MBE and RMSE are statistical quantities to characterize the similarity/differences between two data series. The relative MBE indicates the tendency of one data series to be larger or smaller than the other. The RMSE indicates how far one data series “fluctuates” around the other.

Table 3 shows MBEs and RMSEs for all three Radiance models To be able to directly compare results with Mardaljevic’s validation study for a clear glazing[5], 15 minute

averages of measured illuminances and exterior irradiances have been used as the basis for this table (see below). This reduced the overall number of sky conditions to 814. The table shows that for work plane and ceiling sensors the overall relative MBE and relative RMSE fall for rising model complexity, i.e. simulation results become more accurate as one progresses from $trans_{24\%}$ via $trans_{16\%}$ to *transdata*. As one would expect, the largest improvement comes from $trans_{24\%}$ to $trans_{16\%}$, since the former model overestimates the direct hemispherical transmittance of the translucent panel for all incoming daylight with the exception of rays incident normal to the facade. As in Reinhart's and Walkenhorst's[15] earlier study, errors are larger for the ceiling mounted sensor than for the work plane sensor.

Figure 8 presents the frequency distribution of the relative error, MBE, and RMSE for the facade and the five indoor illuminance sensors for the *transdata* model. Figure 8 is divided into two columns: The left column shows unmodified Radiance simulations. As discussed above, the resulting relative errors are a combination of errors introduced by Radiance and the sky model. In the right column, simulation results from the left have been scaled with a correction factor that equaled the ratio of measured to simulated facade illuminance. The objective of the right column is to estimate the relative weight of simulation errors due to the sky model and surrounding landscape compared to errors from the raytracing.

The figure reveals that for the unmodified Radiance simulations, errors range from 0% to 9% (MBE) and 14% to 19% (RMSE) which is even better than the 8% to 17% (MBE) and 24% to 30% (RMSE) found by Reinhart and Walkenhorst[15] for a clear glazing. The remaining errors due to the raytracing alone (right column) ranged from 1% to -8% (MBE) and 8% to 10% (RMSE), respectively. Again, these values compare well with the

range of –3% to 12% (MBE) and 11% to 20% (RMSE) found by Mardaljevic[5] for a clear glazing.

Practical considerations

The results from the previous sections indicate that one can expect state-of-the-art daylight simulations of different facade geometries including translucent panels to roughly lie within a ±20% error band with respect to "reality"[**]. About half of this error can be attributed to the sky model and practical limitations as to how accurately the surrounding landscape can be modeled. At first sight, these errors might seem substantial. On the other hand, it is worthwhile to remember that the sensor that ultimately judges the appearance and brightness of a daylit space is the human eye, a logarithmic sensor. While a difference between 400lux and 500lux (20%) might not be obvious to the human eye, a difference between 400lux and 4000lux clearly is. The resolution of a daylight simulation is therefore sufficient as far as the human eye is concerned. To provide some further insight into how significant a 10% or 20% error in illuminance predictions is for design purposes, some key daylighting performance measures are calculated in the following based on these error margins.

Figure 9 shows the error bars associated with a ±10% uncertainty in either direction for the daylight factor distribution in the test room used in this validation study (Figure 4). An error of 10% has been chosen, since the daylight factor is based on an idealized CIE overcast sky, which can be exactly modeled by Radiance, i.e. the concept of a sky model error does not apply for daylight factor simulations. For comparison's sake, the daylight factor distribution for the translucent panel is plotted against the distribution for an identical room equipped with a standard tinted double-glazing of 30%

[**] 76% to 86% of all simulations in Figure 8 fall within a ±20% relative error band with respect to measurements.

transmittance. It becomes apparent, that even in a worst case scenario (translucent panel overestimated by 10%; tinted glazing underestimated by 10%) the differences between the two facades remains clear cut in the simulation. If one were to use the US Green Building Council's LEED 8.1 criteria for daylighting (http://www.usgbc.org/) in order to evaluate how far into the room a daylight factor of 2% is maintained, one would find that the width of the daylit zone ranges from about 1.1 m to 1.4 m for the translucent facade and 1.8 m to 2.1 m for the tinted glazing. The uncertainty in the simulation results does not compromise the simulation's ability to contribute to a more informed design decision.

Figure 10 corresponds to the previous Figure except that the daylight autonomy in the two rooms is calculated instead. The daylight autonomy at a point of interest in a building is defined as the percentage of the occupied times per year when the minimum illuminance level can be maintained by daylight alone[15]. In case the building features a movable shading device, the daylight autonomy takes the occupant's use of this shading device into account in order to provide an estimate of how much daylight will effectively be available within the space. It is therefore an holistic daylighting performance indicator that takes occupant needs and the annual dynamics of daylighting into account. In Figure 10, the test reference year for Ottawa, Canada, has been used. The office is continuously occupied Monday through Friday from 8:30 to 16:30. It is assumed that the occupant performs a task that requires a minimum illuminance level of 450lux and is seated at about 2m distance from the facade. The room with the tinted glazing is equipped with perforated roller blinds with a transmission of 5%. Two manual control scenarios are considered for the roller blinds:

- active user: a user who opens the blinds in the morning (upon arrival), and lowers them when direct sunlight above 50 Wm^{-2} hits the seating position (to avoid direct glare). The user further operates the electric lighting in relation to indoor daylight

levels and occupancy patterns based on a number of probability functions that were extracted from field study data[23].

- passive user: a user who keeps the blinds lowered throughout the year to avoid direct sunlight. The user further keeps the electric lighting switched on throughout the working day.

The terms “active” and “passive” user have been taken from the Lightswitch user behavioral model which is based on field data collected in private and two person offices[23].The assumed daylight simulation error from Perez/Radiance in Figure 10 is 20%.

Figure 10 suggests that –if the use of a roller blind is taken into account – the annual daylight availability in the room with the translucent panel is actually larger than in the room with the tinted glazing for both user types. This finding contradicts the results from the daylight factor analysis and might initially seem surprising since the transmittance of the tinted glazing is 0.30 compared to the mean direct hemispherical transmittance of 0.16 for the translucent panel. The key assumption underlying Figure 10 is that it is acceptable for office workers to work in the room with the translucent panel *without* the need for additional shades to mitigate glare. This assumption is supported by a human subject study that was carried out in the two test rooms[24]: During the experiment the rooms were furnished as 2-person shared offices with each occupant facing 45 degrees left or right relative to the façade. “Lighting Quality and Bothersome Glare ratings [...] showed that the higher illuminances were not perceived to be problematic: For the 41 participants in this counterbalanced repeated-measures design, the median overall Lighting Quality rating (scale of 0-4, higher scores indicate higher quality) for Room A was 3,0 and for Room B was 2,8; for Bothersome Glare, both medians were 0,5 (higher scores indicate more bothersome glare, range 0-4).”[24]

Same as for the daylight factor simulation, the simulation uncertainty is always smaller than the differences between the investigated two designs.

Finally, Figure 11 predicts annual electric lighting use in the two rooms from Figure 10. The simulated electric lighting system has an installed lighting power density of 10 Wm^{-2} and is manually controlled with an on/off switch. The dimming system has an ideally commissioned photosensor-control with a ballast loss factor of 10 percent. Simulation results are presented for both rooms for an active and a passive user. In the room with the tinted glazing, the occupant controls both, the light switch as well the blinds whereas in the room with the translucent panel the user only controls the light switch since there are no blinds. The error bars correspond to daylight simulation errors of ±20%. Again, the manual control of the on/off light switch is modeled according to Lightswitch[23].

As for the previous two figures, Figure 11 reveals that the uncertainty introduced through daylight simulation errors is small compared to occupant behavior and facade design. Note, that while the predicted electric lighting use is similar for both rooms for an active user, it is substantially higher for a passive user in the room with the tinted glazing. Since the difference is comparable to the error bars, the projected lighting energy use for active users for both rooms should be considered the same as far as the simulation is concerned. A key finding from Figure 11 is that a translucent panel combined with a photocell controlled dimming system is leading to low lighting energy use *independent* of occupant behavior. The reason is that no shading device can be permanently lowered to reduce the daylight in the room. This suggests that this combination yields more reliable energy savings than a photocell control combined with a standard window and blinds. Once again, this conclusion strongly depends on the assumption that no additional

shading device is needed at any time of the year to mitigate glare form the translucent panel.

4 Discussion and Conclusion

4.1 Radiance validation of a translucent panel

The previous section clearly revealed that Radiance is fully capable of simulating the short time step dynamics of indoor illuminances due to daylight for a design that features translucent panels. Using a *transdata* model based on integrating sphere and goniophotometer measurements yielded MBEs below 9% and a RMSEs below 19% for all desktop and ceiling sensors considered. These simulation accuracies are superior to the 17% (MBE) and 30% (RMSE) that were earlier reported for standard *glass*, *plastic*, and *metal* material types[15]. One explanation why simulations of a translucent material are more accurate than those involving clear glass might be that sharp indoor illuminance gradients (e.g. shadows generated by direct sunlight) are mitigated through translucent panels.

Scaling the simulation results of indoor illuminances with a ratio of measured to simulated facade illuminances reduced the errors to less than -8% (MBE) and 10% (RMSE), suggesting that parts of the simulation errors were introduced by the sky model and surrounding landscape.

The analysis procedure of how to develop a Radiance model from direct hemispherical transmittance and BTDF data described in sections 2.1 and 2.2 can be used for all materials that can be treated as rotationally invariant, diffuse transmitters. In case a material is a diffuse transmitter but not rotationally invariant, the function files in section 2.2 for *transdata* would have to be modified accordingly.

4.2 Goniophotometer and/or integrating sphere measurements

The goniophotometer measurements were useful to establish that the investigated translucent panel could indeed be treated as an ideal diffuser and to quantify diffuse and specular reflectances. Because of the low transmittance of the material and its highly diffusing optical properties, the values determined for the angular dependent direct-hemispherical transmittance deduced from BTDF data had to be verified with additional integrating sphere measurements.

These findings reveal the advantages offered by a combination of two assessment methods to ensure reliable data. Although goniophotometer measurements should a priori be able to provide both an insight into angle-dependent transmittance properties of a sample and integrative, direct-hemispherical measurements, these particular borderline conditions made it beneficial to conduct additional integrating sphere measurements so that integrated BTDF data could be scaled with integrating sphere measurements.

4.3 Radiance material database

A caveat of the findings in this study is that most design practitioners do not have access to the expertise and funding required to commission goniophotometer and integrating sphere measurements of a translucent building product or to develop a Radiance model based on such measurements. This might lead to situations in which a design team refrains from using a translucent panel or fritted glass because the performance of the product cannot be sufficiently well quantified compared to those of conventional glazings. It is therefore in the interest of manufacturers of translucent products to provide Radiance material models on their web site ready for download. An even more rigorous approach, that allows for some quality control, would be to store such

data centrally in a database. Such a database could be added to existing databases such as the "International Glazing Database" that forms part of the Window software[*]. Note that Window 5.2 already provides an export function for complex glazings (albeit not validated) to Radiance.

4.4 Use of "transdata" to model photosensors

Section 3 demonstrated that *transdata* is a flexible Radiance material type to adjust the angular transmittance properties of a material. It actually offers an alternative approach of how to model the spatial sensitivity distribution of real world photosensors within Radiance to the approach suggested by Ehrlich *et al.*[25]: Instead of folding a Radiance image of a room as "seen" by the photosensor with an image of the photosensor's spatial sensitivity, this new approach would be to place a "filter" polygon in front of the photosensor. This filter, modeled with a function file material, could modify the angular sensitivity of the sensor from a cosine dependency to an arbitrary function. The advantage of this approach would be that the performance of photocell controls could be investigated on an annual basis using a daylight coefficient approach.

Summing up, this study once more demonstrated the flexibility that a Perez/Radiance/daylight coefficient approach offers to model the annual daylight availability in a building. The results also show that careful BT(R)DF measurements combined with integrating sphere measurements are an excellent way to develop accurate but easy-to-use material models for daylight simulations. The simulation accuracy reached in this study translated into small error bands for daylight performance measures such as daylight factor and daylight autonomy that were derived from these

[*] http://windows.lbl.gov/software/window/window.html

simulations. This suggests that the simulation accuracy that is currently reached by Radiance is sufficient for practical design considerations. A remaining task will be to provide a larger group of design professionals with the skills and data required to carry out such daylight simulations. A central material database could be one step towards this goal. Another challenge for the research community will be to help design professionals to translate detailed simulation results into compact and intuitive daylighting performance measures. This task will require further research on building occupants' perception of and relationship with the indoor environment well as on the design decision process itself.

Acknowledgement

This work has been funded by Kalwall (Keller Company), the National Research Council Canada under the contract number B3223, the Swiss Federal Institute of Technology (EPFL) and the Commission for Technology and Innovation (CTI). The authors are indebted to Roger Marchand for preparing the NRC Daylighting Laboratory for the validation measurements. Very special thanks to Greg Ward, the guiding hand behind the development of the *transdata* model used in this study. We are further indebted to Tilmann Kuhn (Fraunhofer ISE) for carrying out the integrating sphere measurements and to Aziz Laouadi and Guy Newsham for providing valuable comments on a draft version of this paper.

References

1. Reinhart C F and Fitz A, "Findings from a survey on the current use of daylight

simulations in building design", Energy and Buildings, (In press 2005).

2. Ward G and Shakespeare R, “Rendering with RADIANCE. The Art and Science of Lighting Visualization”, Morgan Kaufmann Publishers (1998).

3. Ward G J, "Measuring and Modeling Anisotropic Reflection", Computer Graphics, 26 (2), 265-272 (1992).

4. Mardaljevic J, "Validation of a Lighting Simulation Program under Real Sky Conditions", Lighting Research & Technology, 27 (4), 181-188 (1995).

5. Mardaljevic J, "Validation of a Lighting Simulation Program: A Study Using Measured Sky Brightness Distributions", Lux, Conf. Proceed. The 8th European Lighting Conference, Amsterdam 11- 14 May, 555-569 (1997).

6. Mardaljevic J, "Simulation of annual daylighting profiles for internal illuminance", Lighting Research & Technology, 32 (2), 111-118 (2000).

7. Aizlewood M E, "Innovative daylighting systems: An experimental evaluation", Lighting Research & Technology, 25 (4), 141-152 (1993).

8. Tregenza P R and Waters I M, "Daylight Coefficients", Lighting Research & Technology, 15 (2), 65-71 (1983).

9. CIE , "Standardization of Luminance Distribution on Clear Skies", Publication # 022, S003, (1996).

10. Reinhart C F and Herkel S, “The Simulation of Annual Daylight Illuminance Distributions- A state of the art comparison of six RADIANCE-based methods”, Energy & Buildings 32(2), 167-187 (2000).

11. Ng E, “A study on the accuracy of daylighting simulation of heavily obstructed buildings in Hong Kong”, Conf. Proc. of the IBPSA Conference in Rio de Janeiro, Brazil , 1215-1222 (2001).

12. Mardaljevic J, "Verification of program Accuracy for Illuminance Modeling: Assumptions, Methodology and an Examination of Conflicting Findings", Lighting Research & Technology, 36(3), 218-238 (2004).

13. Perez R, Seals R, and Michalsky J, ”All-Weather Model for Sky Luminance Distribution - Preliminary Configuration and Validation”, Solar Energy 50(3), 235-245 (1993).

14. Crawley D B, Hand J W, and Lawrie L K, "Improving the Weather Information Available to Simulation Programs", Sixth International IBPSA Conference (BS '99) Kyoto, Japan, II 529-536 (1999).

15. Reinhart C F and Walkenhorst O, "Dynamic RADIANCE-based Daylight Simulations for a full-scale Test Office with outer Venetian Blinds", Energy & Buildings, 33(7), 683-697 (2001).

16. Hartwig H, "Integration of Thermotropic Layers in Light-Transmitting Building Components", PhD thesis, Technical University Munich, Germany (2003).

17. Murdoch J B, Oliver T W, and Reed G P, "Luminance and Illuminance Characteristics of Translucent Daylighting Sandwiched Panels", Journal of the Illuminating Engineering Society, (Summer), 69-82 (1991).

18. Andersen M, Roecker C, and Scartezzini J.-L, "Design of a time-efficient video-goniophotometer combining bidirectional functions assessment in transmission and

reflection", Solar Energy Materials and Solar Cells , 88(1), 97-118 (2005).

19. Andersen M, "Matrix-based analysis of digital images: application to goniophotometric measurements with variable referential", Optics and Lasers in Engineering, 43(3-5), 419-435 (2005).

20. Andersen M, "Light distribution through advanced fenestration systems", Building Research & Information, 30(4), 264-281 (2002).

21. Andersen M, "Validation of the performance of a new bidirectional video-goniophotometer", Lighting Research and Technology, In Press (2006).

22. ASHRAE, “ASHRAE Handbook – Fundamentals”, American Society of Heating, Refrigerating and Air-conditioning Engineers, Atlanta 2005.

23. Reinhart C F, "LIGHTSWITCH 2002: A model for manual and automated control of electric lighting and blinds", Solar Energy, 77(1), 15-28 (2004).

24. Veitch JA, Tosco A-M, and Arsenault C D, "Photometric issues in healthy lighting research and application", Proc. of the CIE Symposium '04 - Light and Health: Non-Visual Effects, Vienna, Austria, 146-149 (2004).

25. Ehrlich C, Papamichael K, Lai J, and Revzan K, "A method for simulating the performance of photosensor-based lighting controls", Energy and Buildings, 34 883-889 (2002).

List of Table Captions

Table 1: List of materials in Radiance scene.

Table 2: List of Radiance simulation parameters.

Table 3: Mean Bias Error (MBE) and Root mean Square Error (RMSE) for the three Radiance material models.

Table 1:

material	optical properties	Radiance material description
ceiling	86% diffuse reflectance	void plastic ceiling 0 0 5 0.86 0.86 0.86 0 0
carpet	dark patches 10% diffuse reflectance light patches 16% diffuse reflectance => 13% diffuse reflectance	void plastic carpet 0 0 5 0.13 0.13 0.13 0 0
side walls	73% diffuse reflectance	void plastic side_wall 0 0 5 0.73 0.73 0.73 0 0
mullions (unpainted aluminum)	74% diffuse reflectance with a estimated 10% specular component	void plastic moullion 0 0 5 0.74 0.74 0.74 0.1 0
outside gravel	22% diffuse reflectance	void plastic gravel 0 0 5 0.22 0.22 0.22 0 0
external wall	40% diffuse reflectance	void plastic ext_wall 0 0 5 0.4 0.4 0.4 0 0
black cloth covering hedge	~0% diffuse reflectance (approximated value)	void plastic black_cloth 0 0 5 0 0 0 0 0
tinted glazing	31% normal visible transmittance (based on integrating sphere measurements)	# transmissivity in Radiance: 0.338117 void glass tinted_glazing 0 0 3 0.338117 0.338117 0.338117
translucent panel	BTDF measurements	three Radiance models (see above)

Table 2:

ambient bounces	ambient division	ambient sampling	ambient accuracy	ambient resolution	direct threshold	direct sampling
7	1500	100	0.1	200	0	0

Table 3:

sensor		$trans_{24\%}$	$trans_{16\%}$	transdata
DESK1	MBE [%]	49.5	7.5	3.5
	RMSE [%]	52.4	14.6	14.3
CEIL1	MBE [%]	57.7	12.7	8.9
	RMSE [%]	60.9	19.2	18.6

List of Figure Captions

Figure 1: Exterior (a) and interior (b) sides of the analyzed translucent panel.

Figure 2: Visualization of photometric solid[20] examples and section views for various incident directions and characterization modes: (a) BTDF along $\theta_{incident}$=45°, $\phi_{incident}$ =0°, sample Ø = 280 mm; (b) BTDF along 60°, 0°, Ø = 280 mm; (c) BTDF along 45°, 0° (section view), Ø = 280 mm; (d) BTDF along 60°, 90°, Ø = 280 mm; (e) BTDF along 75°, 0°, Ø = 280 mm; (f) BRDF along 20°, 0°, Ø = 150 mm.

Figure 3: Comparison of the directional-hemispherical transmittance properties of the translucent panel measured with a goniophotometer (dotted line) and with an integrating sphere (solid line). The estimated, relative errors of both measurement setups were 15% for the goniophotometer and 5% for the integrating sphere.

Figure 4: (a) Internal view of one of the two test rooms in the NRC Daylighting Laboratory. The tested facade was fitted with a large translucent sandwiched panel and a small view window. (b) External view of the daylighting laboratory and the surrounding "hedge" which was covered with black cloth.

Figure 5: Section of the test room. All five illuminance sensors were positioned along the central axis of the room.

Figure 6: Measured and simulated illuminances for desk sensor Desk 1 (see Figure 5) for a partly cloudy day.

Figure 7: Measured and simulated illuminances on a sunny day for (a) a facade sensor and (b) desktop sensor Desk 1 (see Figure 5). For the facade sensor simulation, results for *trans* and *transdata* are identical.

Figure 8: Frequency distribution of relative error for illuminance predictions using the "transdata" model in Radiance. The left column shows unmodified simulation results. In the right column simulation results have been scaled with the ratio of measured to simulated facade illuminance. The spectra are based on 15 minute averages of measured indoor illuminances and external irradiances.

Figure 9: Daylight factor distribution in the test room equipped with either a translucent panel or a tinted double glazing. The assumed of the underlying daylight simulation is ±10%.

Figure 10: Daylight autonomy distribution in the test room equipped with either a translucent panel or a tinted double glazing with roller blinds. The assumed error of the underlying dynamic daylight simulation is ±20%. (There is only one daylight autonomy distribution for the translucent panel variant, since it does not feature a roller blind.)

Figure 11: Annual electric lighting use for an ideally commissioned photocell controlled dimmed lighting system in the test room equipped with a either translucent panel or a tinted double glazing combined with a roller blind, for an *active* and a *passive* user.

Figure 1:

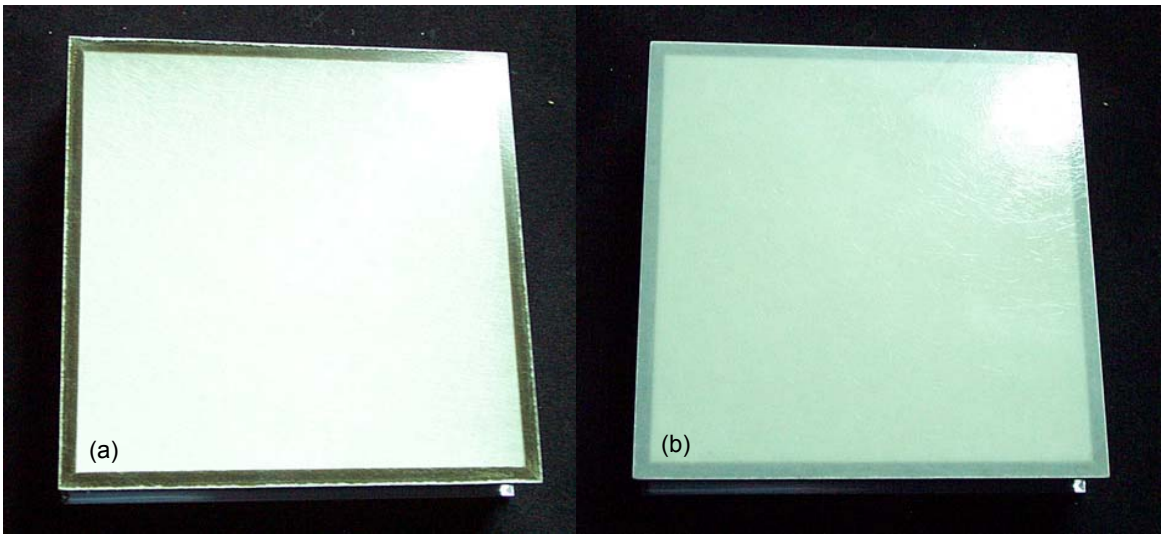

Figure 2:

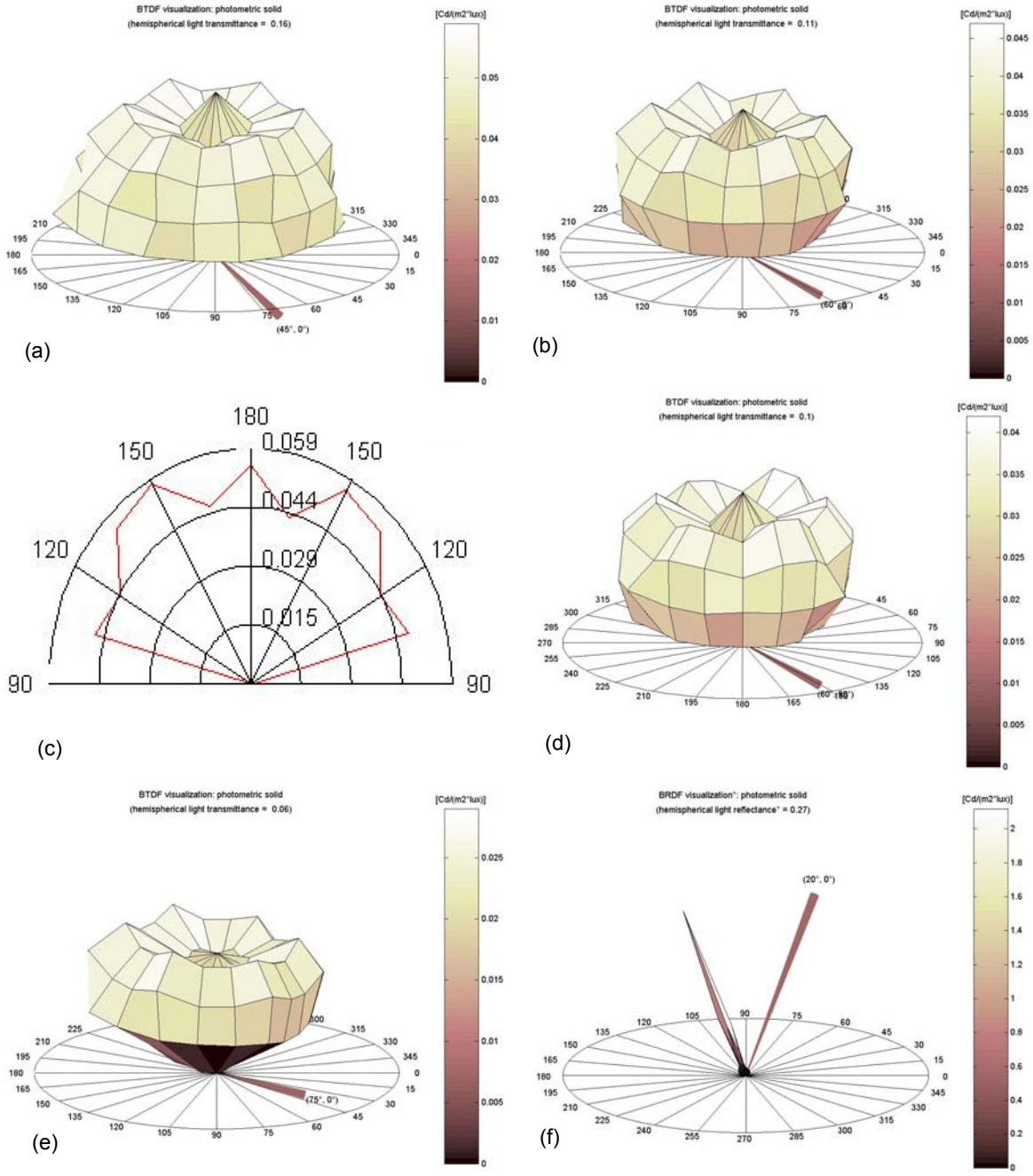
BTDF visualization: photometric solid
(hemispherical light transmittance = 0.16)
[Cd/(m2*lux)]
(45°, 0°)
(a)
BTDF visualization: photometric solid
(hemispherical light transmittance = 0.11)
[Cd/(m2*lux)]
(b)
180
150
150
120
120
90
90
0.059
0.044
0.029
0.015
(c)
BTDF visualization: photometric solid
(hemispherical light transmittance = 0.1)
[Cd/(m2*lux)]
(d)
BTDF visualization: photometric solid
(hemispherical light transmittance = 0.06)
[Cd/(m2*lux)]
(75°, 0°)
(e)
BRDF visualization*: photometric solid
(hemispherical light reflectance* = 0.27)
[Cd/(m2*lux)]
(20°, 0°)
(f)

Figure 3:

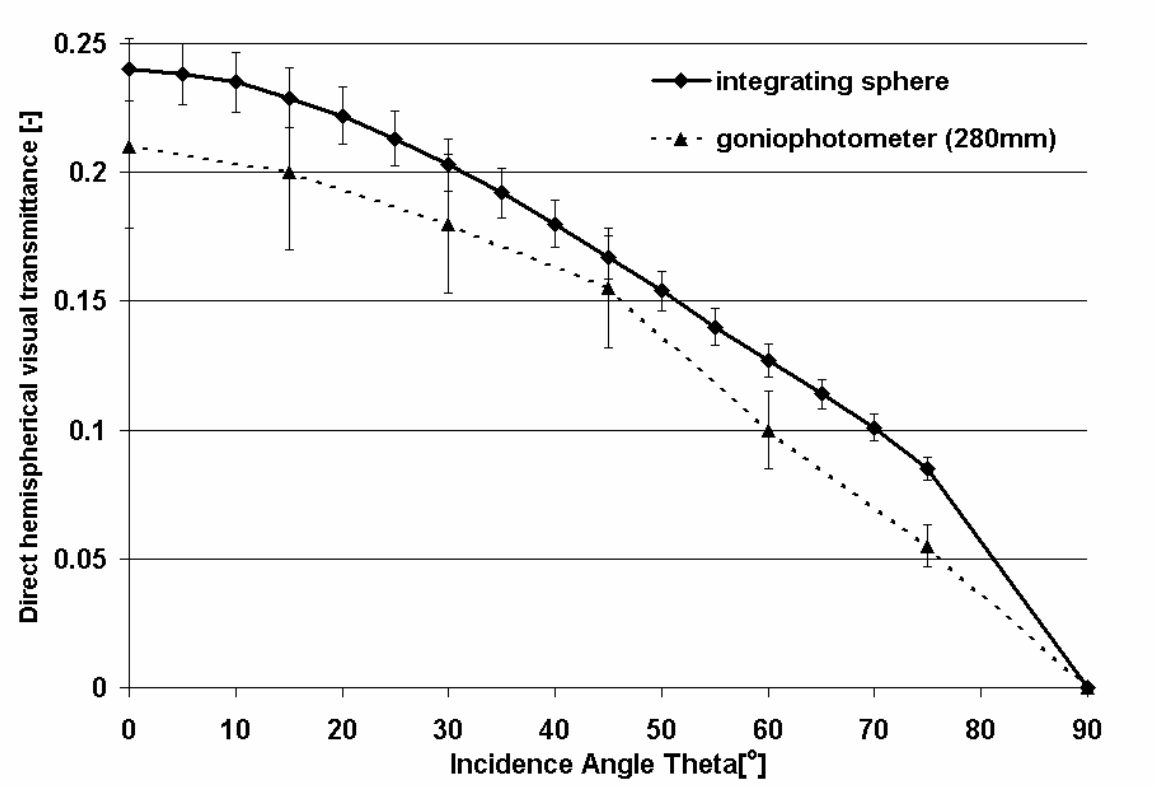
integrating sphere
goniophotometer (280mm)
Direct hemispherical visual transmittance [-]
0.25
0.2
0.15
0.1
0.05
0
0
10
20
30
40
50
60
70
80
90
Incidence Angle Theta[°]

Figure 4:

(a) 

(b) 

Figure 5:

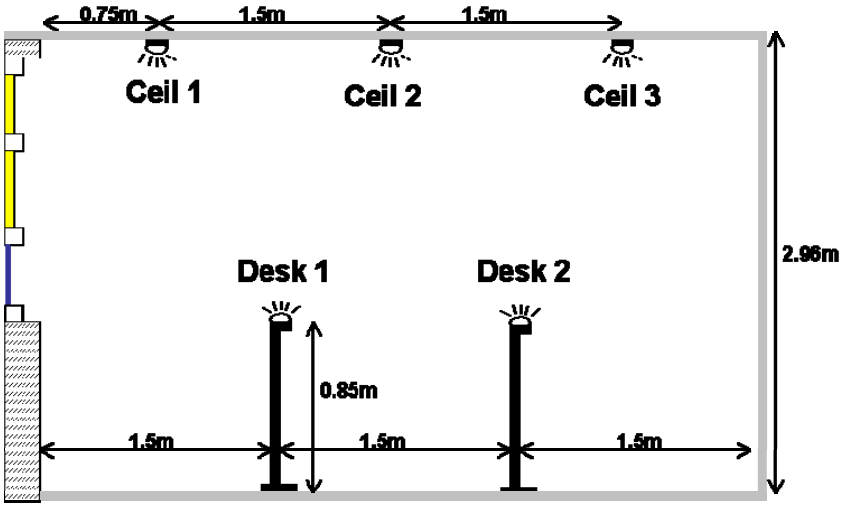
0.75m
1.5m
1.5m
Ceil 1
Ceil 2
Ceil 3
2.96m
Desk 1
Desk 2
0.85m
1.5m
1.5m
1.5m

Figure 6:

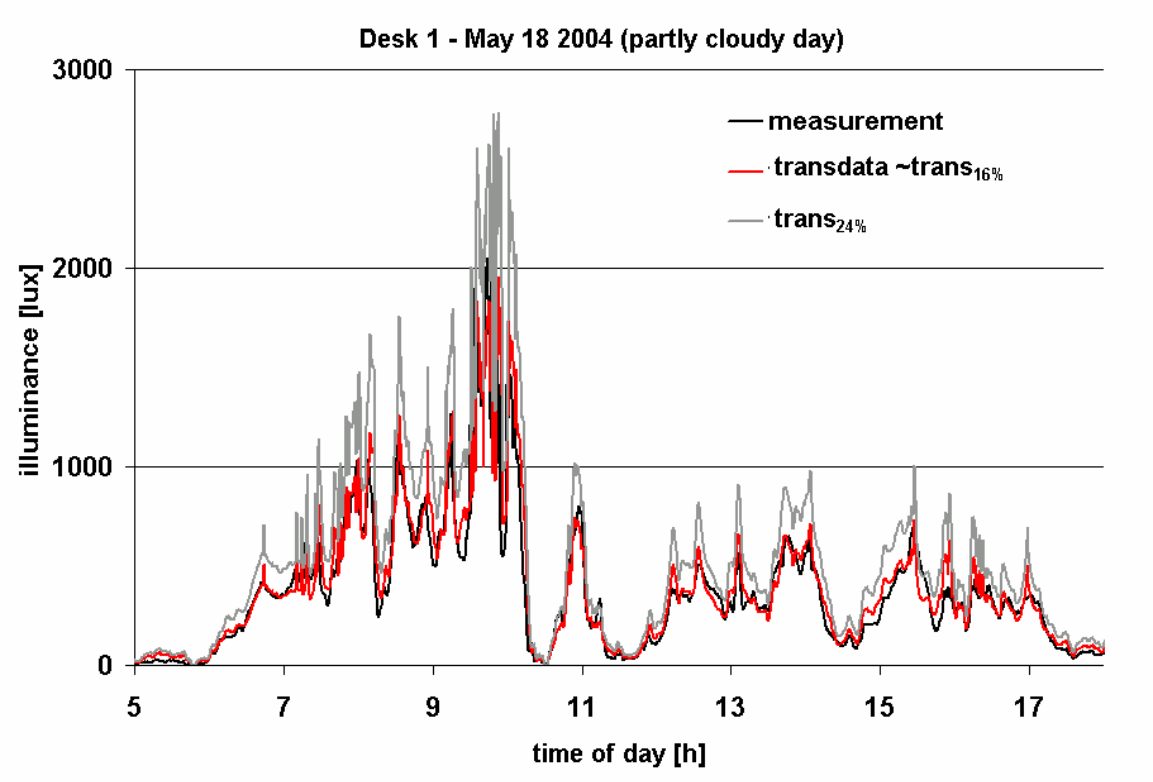
Desk 1 - May 18 2004 (partly cloudy day)
3000
2000
1000
0
illuminance [lux]
5
7
9
11
13
15
17
time of day [h]
measurement
transdata ~trans16%
trans24%

Figure 7 (a):

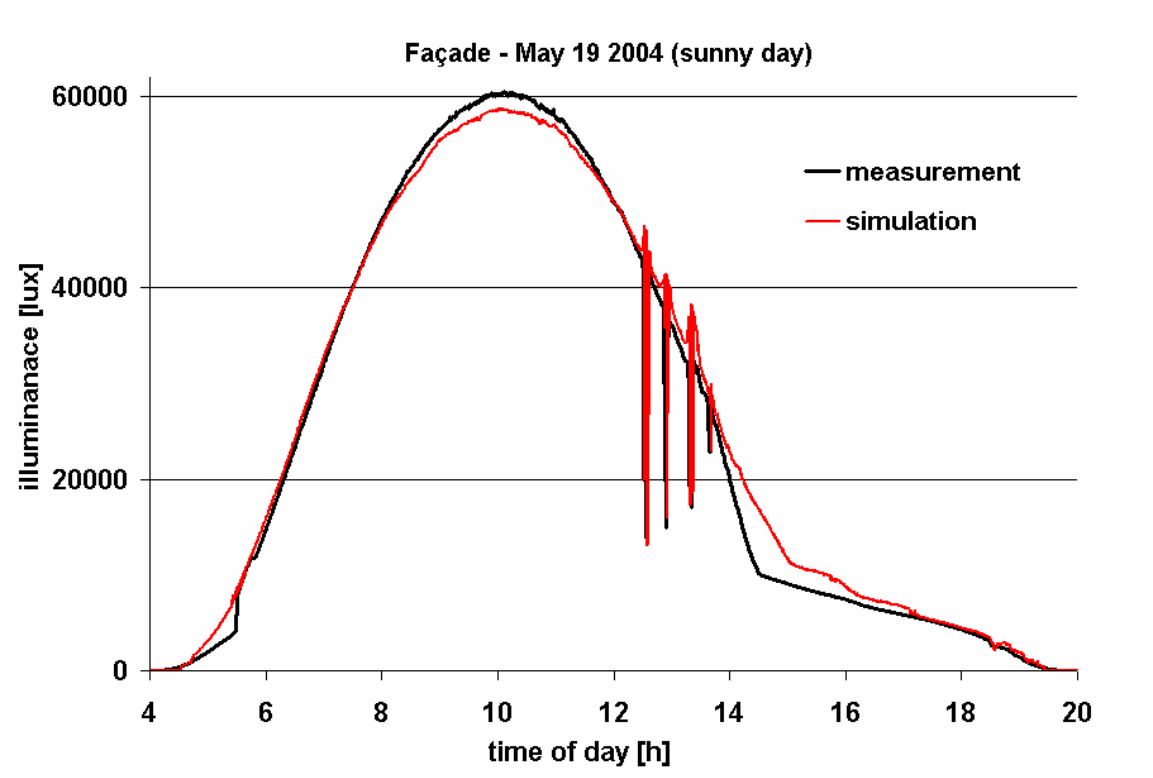
Façade - May 19 2004 (sunny day)
60000
40000
20000
0
illuminanace [lux]
4
6
8
10
12
14
16
18
20
time of day [h]
measurement
simulation

Figure 7 (b):

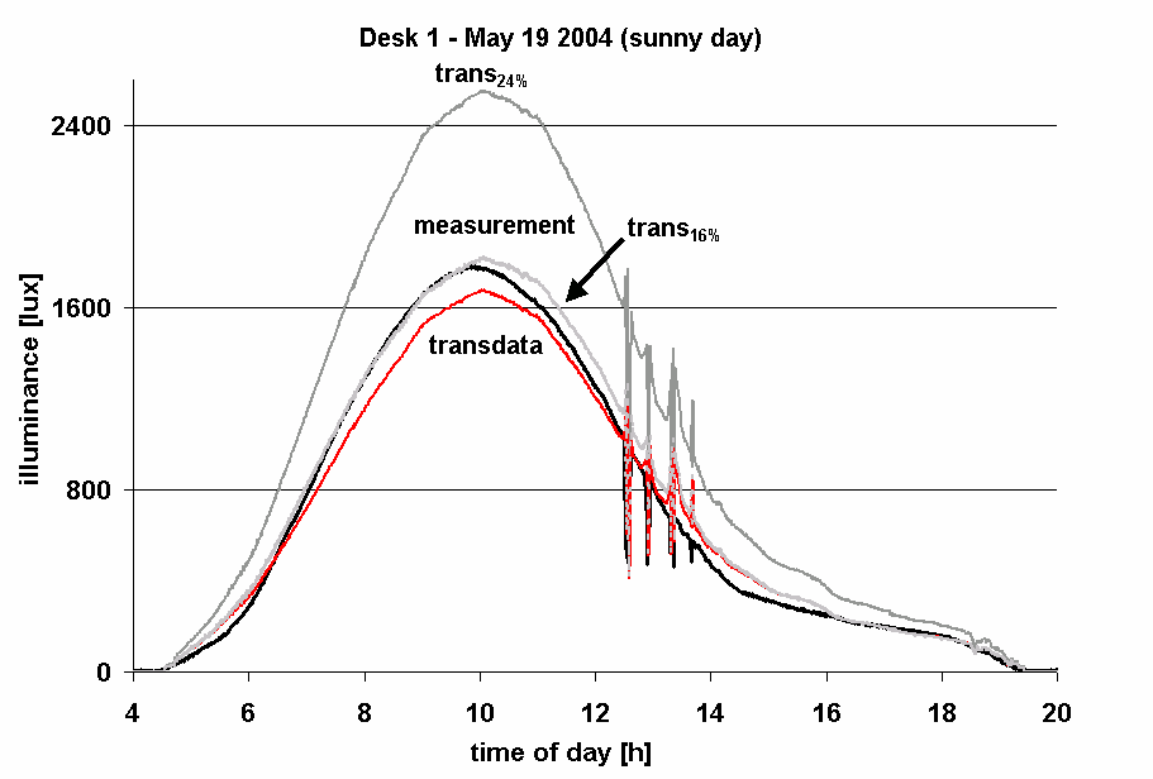
Desk 1 - May 19 2004 (sunny day)
trans24%
2400
measurement
trans16%
1600
transdata
800
0
illuminance [lux]
4
6
8
10
12
14
16
18
20
time of day [h]

Figure 8:

unmodified Radiance simulation	corrected Radiance simulation
(a) facade illuminance	
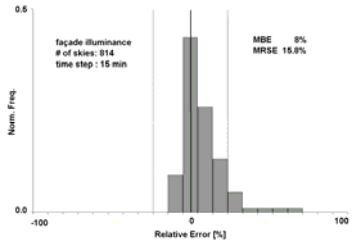	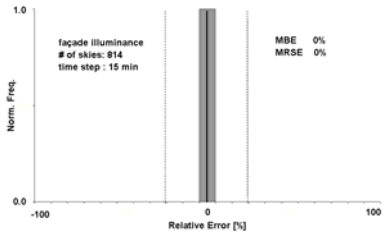
(b) desk sensor near facade	
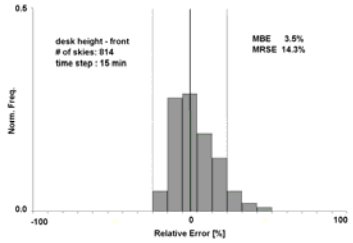	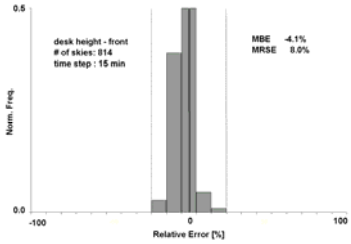
(c) desk height back of the room	
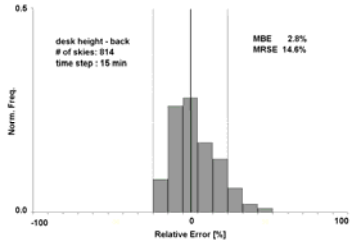	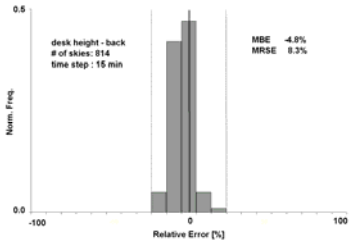
(d) ceiling sensor near facade	
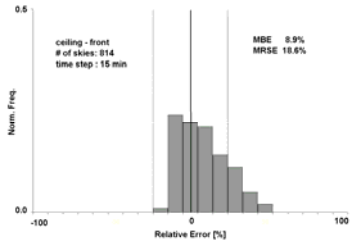	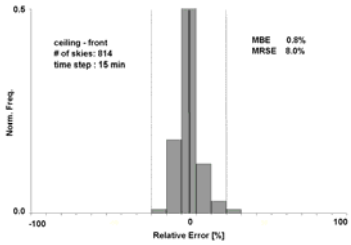
(e) ceiling sensor back of the room	
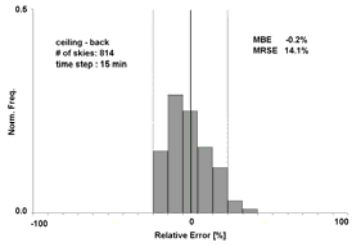	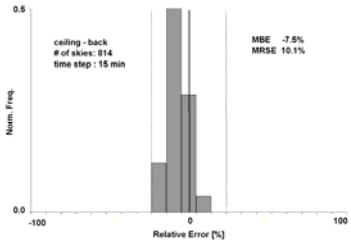

Figure 9:

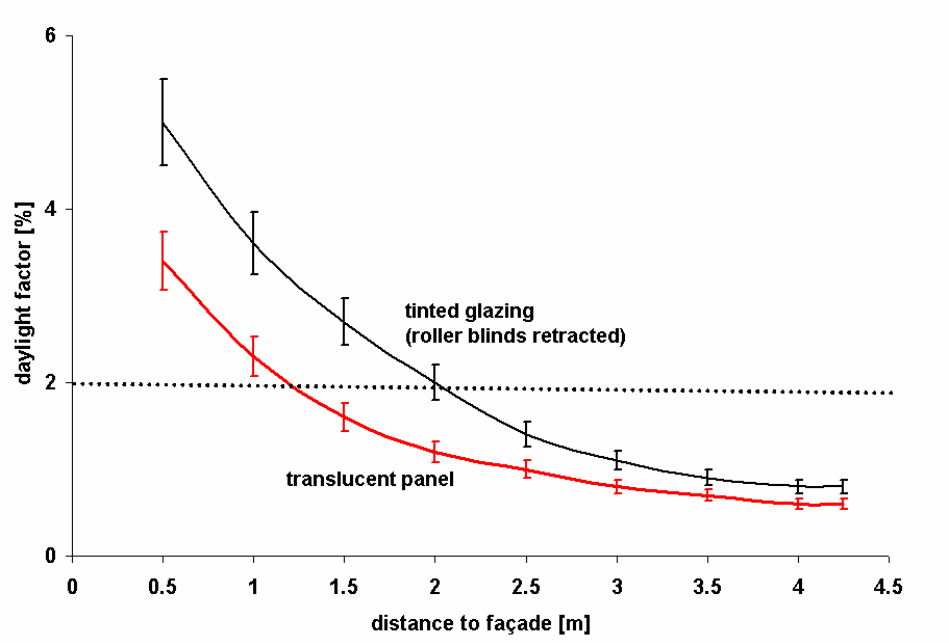
6
4
2
0
daylight factor [%]
tinted glazing
(roller blinds retracted)
translucent panel
0
0.5
1
1.5
2
2.5
3
3.5
4
4.5
distance to façade [m]

Figure 10:

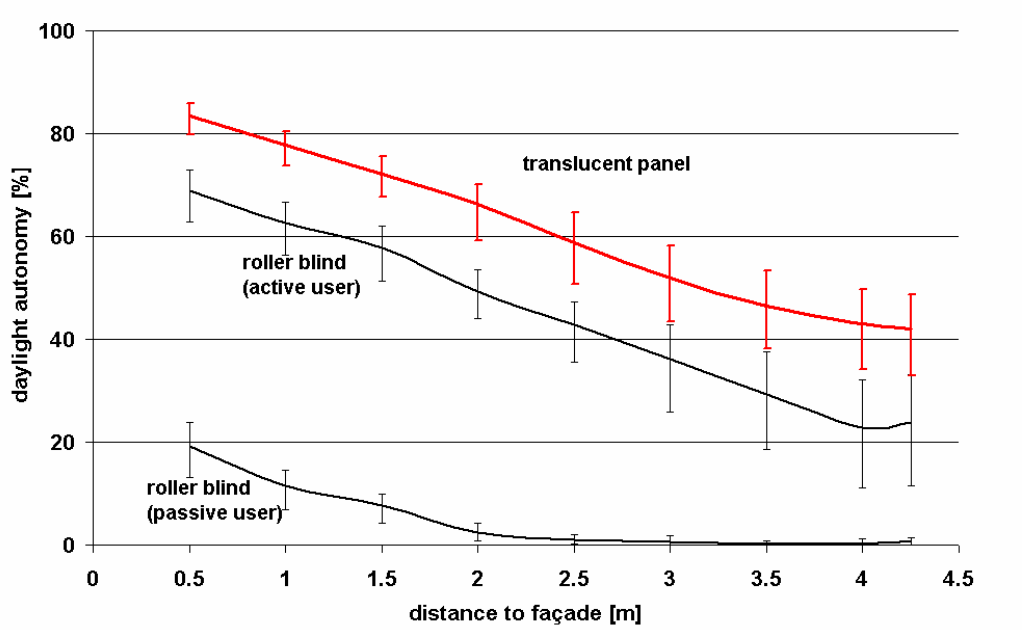
100
80
60
40
20
0
daylight autonomy [%]
translucent panel
roller blind
(active user)
roller blind
(passive user)
0
0.5
1
1.5
2
2.5
3
3.5
4
4.5
distance to façade [m]

Figure 11:

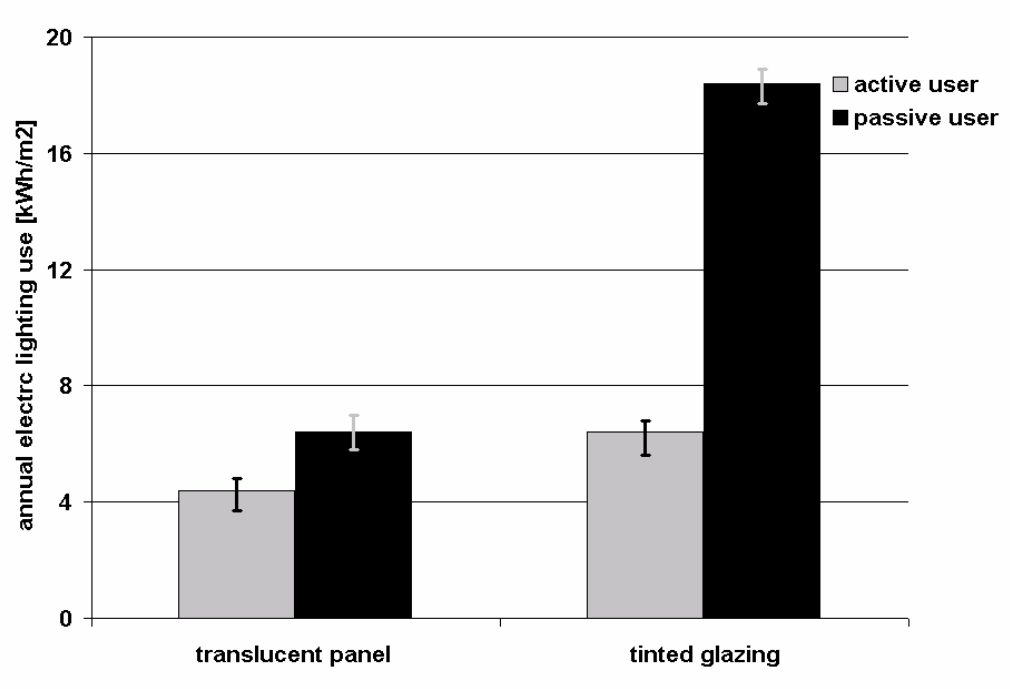
20
16
12
8
4
0
annual electrc lighting use [kWh/m2]
active user
passive user
translucent panel
tinted glazing